AN1463

NiMH Trickle Charger with Status Indication

Authors: *Siva Periasamy*
Tony O'Byrne
Microchip Technology Inc.

INTRODUCTION

In spite of the considerable media attention to the concept of recyclable power sources, usage of rechargeable Nickel-Metal Hydride (NiMH) cells has been limited. The combined charger and cell cost have been a mitigating factor in favour of primary cells. The high internal impedances of primary cells are not suitable for the surge currents needed for digital cameras, DC motors and walkie-talkies. NiMH cells exhibit low internal impedances and, as such, are particularly viable in these applications. The digital camera user may be more discerning about using the NiMH batteries, but the toy market is still dominated by the primary cells solely due to cost considerations. In the long run, rechargeable batteries are more cost-effective. Commercial NiMH chargers can be classified into two areas:

a) Fast chargers that take 15 minutes to three hours to charge two or four cells.

b) Trickle chargers that take about 15 hours to charge two or four cells.

Note 1: A cell is a single physical unit with an anode and cathode to produce the rated voltage. A battery can be a single cell, or a group of multiple interconnected cells to produce the required voltage. The term cells and batteries are used interchangeably in this application note.

2: A battery's capacity is measured in Ampere-hours and the C rate is the current which a battery delivers if it is completely discharged in one hour. For instance, a 2000 mAH battery, charged at 200 mA, is said to be charged at 0.1C rate.

PROFILES OF NiMH BATTERIES UNDER VARIOUS CHARGE CONDITIONS

Figure 1 shows the charge efficiency at different charge rates. This is a variable quantity dependant on the state of charge and the charging current. The maximum charge efficiency is seen at charge rates between 0.5C and 1C. The details of this data are beyond the scope of this application note, and additional information is available in the listed references.

FIGURE 1: CHARGE EFFICIENCY AT DIFFERENT CHARGE RATES

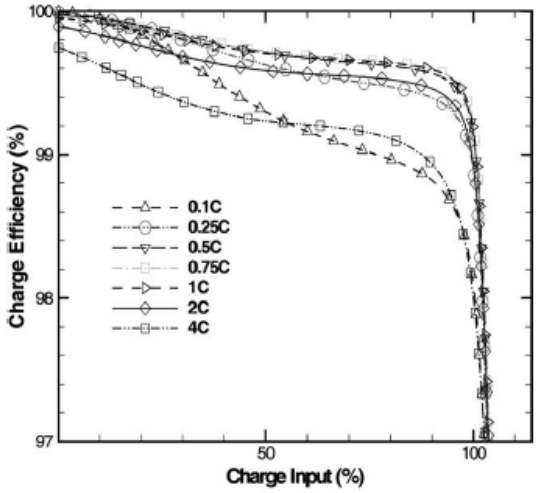

During the charging and overcharging process, oxygen is generated at the nickel electrode. This oxygen recombines with the metal hydride electrode, thereby preventing the build-up of cell pressure. However, at high charge currents, the rate of oxygen generation may exceed the recombination process. The accompanying thermal build up and accumulation of oxygen will lead to cell pressure build-up leading to cell damage and the electrolyte will leak out of the case. Details of this electrochemical reaction are available in the **Section "References"**. Figure 2 shows the cell pressure profiles at various charging rates.

FIGURE 2: CELL PRESSURE PROFILES AT VARIOUS CHARGING RATES

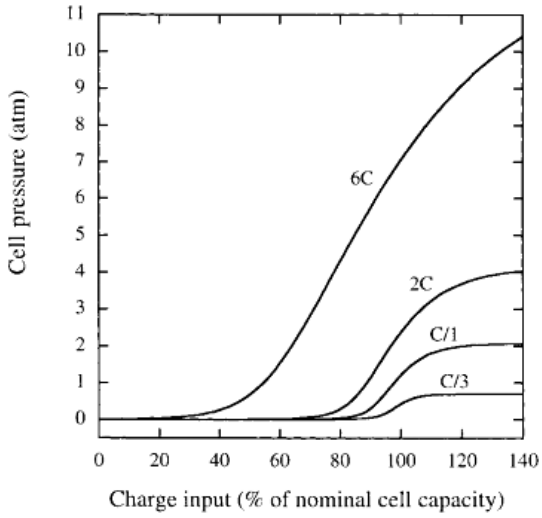

FAST CHARGERS

Fast chargers employ a constant-current charge management algorithm with charge currents from 0.5C to 6C, and are often based on switch-mode controllers. The design would involve consideration to temperature management, EMI and safety. In view of the large charge currents and build up of cell pressure, as seen in Figure 2, detection of the charge status and cut-off is crucial to avoid cell and charger damage. EMI, safety compliance testing, materials procurement, manufacturing complexity and test complexity add additional costs. Typically, the charge management algorithm would detect charge completion and change the charge profile to a lower charge current, while monitoring for faulty batteries. The following conditions are detected and displayed visually:

- Charge completion
- Insertion of primary cell
- Insertion of a fully charged battery
- Insertion of a shorted cell

The algorithm can charge a partly discharged battery without overcharging it. Some chargers may have additional features to detect special NiMH cells which can handle high charge currents.

A visual display in the form of LEDs or LCDs with an audible alarm may be implemented. The reader can refer to the references at the end for schematics and details of these chargers.

Their higher cost limits their sales to the more discerning customer.

TRICKLE CHARGERS

Commercial trickle chargers do not have any charge management algorithm and the typical charge currents are limited to 0.1C or lower. The charge current is limited by a resistor in conjunction with the transformer impedance, as seen in Figure 3, which also explains the basic concept of a trickle charger.

FIGURE 3: TRICKLE CHARGER

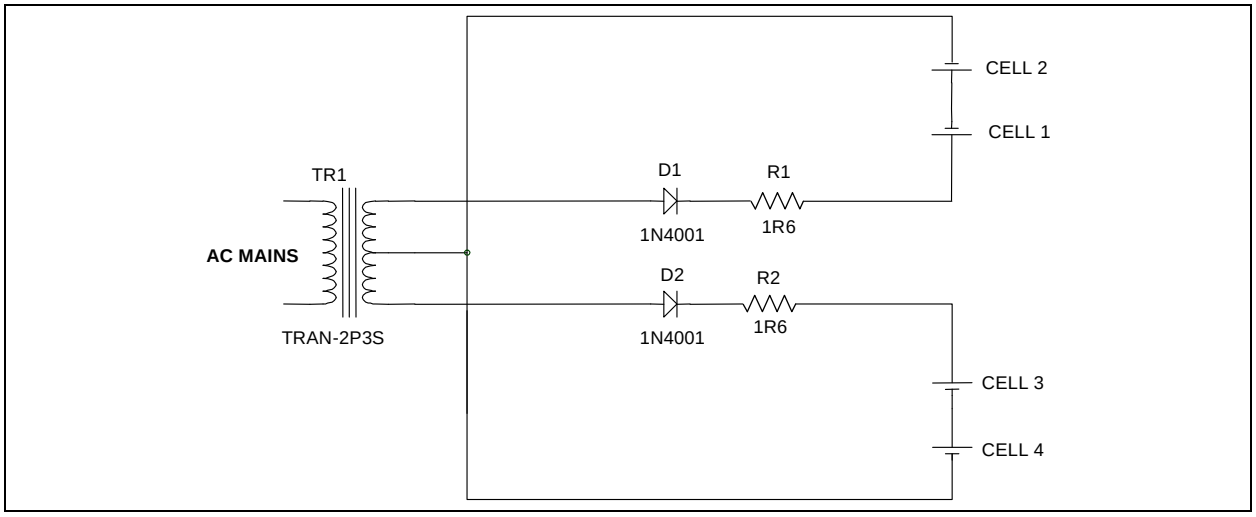

This dual channel charger is cheap, uses very few components and the charge current is approximately 0.1C or lower.

Resistors R1 and R2 limit the charge current to the AA cells to approximately 0.1C. Batteries are charged overnight, and the user is expected to remove the cells from the charger after the charge duration. A simple circuit to light LEDs can be added to indicate that the charger is working.

TECHNICAL LIMITATIONS

a) Inability to detect a primary cell insertion
b) Inability to detect defective cells
c) No clear indication that 15 – 16 hours of charge duration has been completed. In most commercial chargers, the LED does not turn off.
d) Insertion of fully charged or partly charged cells is not detected. As such, overcharge and subsequent damage to the NiMH cells is possible.

INTELLIGENT TRICKLE CHARGER DESIGN

This application note describes a low-cost microcontroller-based trickle charger, that overcomes the prevailing limitations in low-cost trickle chargers by providing intelligence related to charge status and Fault conditions. The document also discusses the use of statistical techniques to develop a robust algorithm resilient to the variation in the measured values. The proposed design allows four NiMH batteries to be charged simultaneously.

The fact that it uses very few components makes it inherently more reliable than a fast charger. The low-charge current facilitates oxygen recombination and the cell pressure will never reach catastrophic levels. As such, it is not necessary to add additional safety circuitry. Moreover, compliance to international safety and emission requirements is easier, as it does not use any switched mode power supplies. A normal 50 or 60 Hz transformer is used to step down the mains voltage. The manufacturing complexity is very low, as it uses commonly available components.

DESIGN SPECIFICATIONS

Table 1 outlines the specifications for a low-cost, two-channel intelligent trickle charger.

TABLE 1: CHARGER DESIGN SPECIFICATIONS

Characteristics	Specification		Comments
Input Voltage	Nominal	230V, 50Hz	+5% -10%
	Operation	207V – 241V	
Output Voltage	Nominal	3.0V DC	No load voltage
Input Protection	Thermal resistor in transformer		
Output protection	Current limit resistor in conjunction with the transformer's impedance and thermal cut-off resistor built into the transformer.		
Display Functionality	**Function**		**LED Status**
	Battery not present		OFF
	Battery present. Charging		ON
	Charge completed		Flash slowly at a rate of 1-2 seconds
	Faulty Battery		Flash fast at a rate of 100-200 milliseconds

The schematic of the proposed charger is shown in Figure 4.

FIGURE 4: SCHEMATIC OF THE INTELLIGENT TRICKLE CHARGER

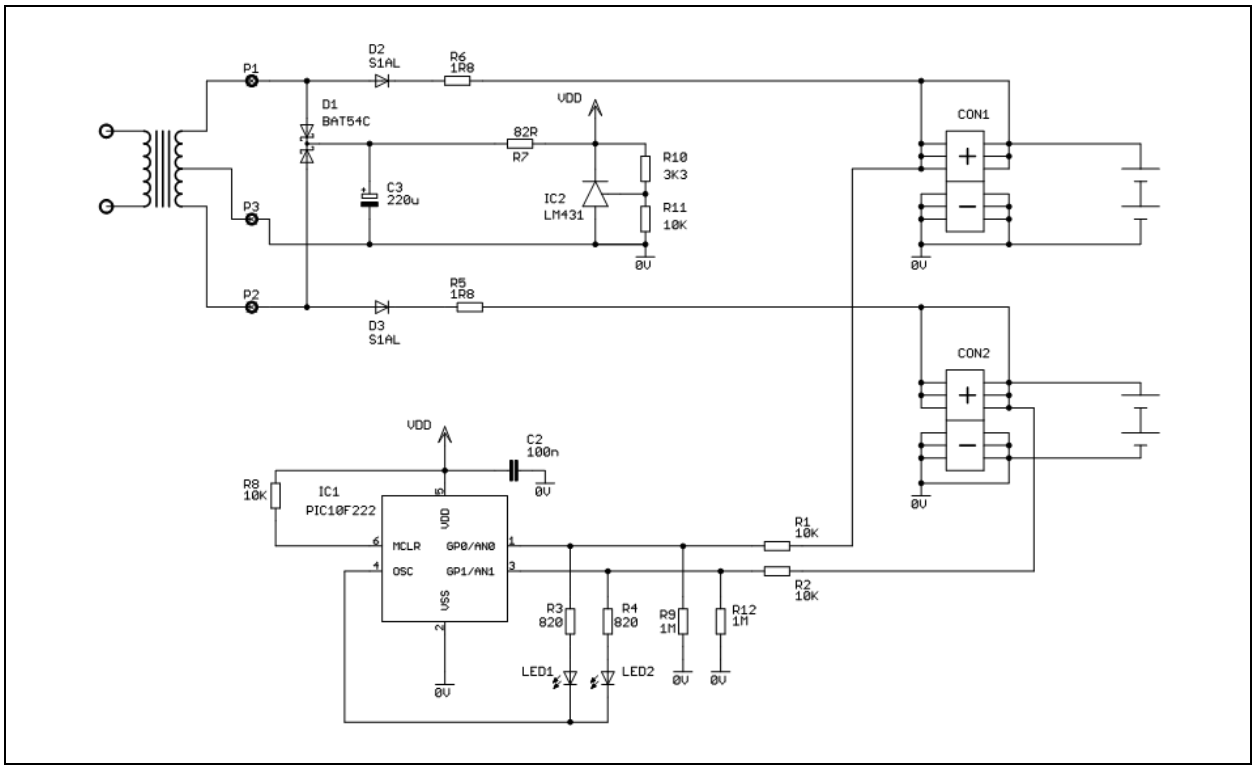

The charger circuit consists of two half-wave rectifiers charging the two series connected cells in each channel. The following calculations represent the nominal values. In reality, the charge current will vary due to the fluctuations in the mains supply, transformer impedance, the battery's residual charge, battery impedances and environment conditions.

The PIC10F222 was chosen due to the small form factor and cost. It has three input/output ports and one input-only port. The internal oscillator is set to 4 MHz, and Timer0 is used as the base clock for the algorithm and the internal Analog-to-Digital Converter is used for measuring the battery voltages.

Pins GP0 and GP1 are used to measure the battery voltages, as well as drive LEDs, in conjunction with GP2. Prior to the ADC measurement, GP2 goes to High and disables LED1 and LED2. After the measurements, GP2 goes to Low to enable the LEDs.

R5 and R6 are current-limiting resistors. Resistors R1 and R2 provide the source impedances to the Analog-to-Digital Converter. They also stop the batteries from powering up the PIC® device via the internal protection diodes. Resistors R10 and R12 are needed to ensure stable voltage readings when pins GP0 and GP1 switch from digital, analog or High-Impedance mode.

The PIC device does not manage the charging process. It provides the intelligence and visual indication to the user to overcome the limitations of an analog trickle charger.

CHARGE STATUS DISPLAY

Table 1 shows the display functionality to indicate the charge status with the current software. More complex LED flashing sequences are possible by changes to the display routine.

The charging starts when the charger is plugged into the mains, and stops when the charger is removed. A power recycle, by removing the charger from the mains socket to reset the PIC device, is required if a faulty battery is detected.

CALCULATIONS

Ignoring the power consumption of the electronic components, the overall efficiency of the charger can be calculated.

- Fractional VA rated transformer efficiency is typically 75%.
- Half-Wave rectifier efficiency is 40%
- Battery charge efficiency at 0.1C is 98%.

The overall efficiency of this charger is therefore (Equation 1):

EQUATION 1:

$$\eta = 0.75 \times 0.4 \times 0.98 = 29\%$$

Even though the charge efficiency is 29%, the lower cost with the added intelligence will make this an attractive proposition.

Fractional VA-rated transformers are small transformers used in consumer appliances. The primary current is less than 1 amp, and these transformers exhibit poor voltage regulation. The figures below show the measured values in the prototype unit tested.

Secondary Peak Voltage: Vp = 10.0V (no load)

Secondary Peak Voltage: Vp = 8.1V (full load)

This translates to rms values of 7.07V and 5.73V, respectively.

EQUATION 2: TRANSFORMER REGULATION

$$Transformer\ Regulation = \frac{Vno_{load} - Vfull_{load}}{Vfull_{load}}$$

The transformer regulation was calculated to be 23.4% and must be factored into the design.

The average voltage V_{DC} after the diode drop is given by the equation below.

EQUATION 3: DC VOLTAGE

$$V_{DC} = \frac{\tilde{Vm}}{\pi} - 0.7$$

Where

V_{DC} = DC voltage

Vm = Peak value of the AC voltage

The values below were thus calculated:

EQUATION 4:

$$V_{DC_{noload}} = 2.5 Volts$$

At first glance, it appears that the calculated average voltage is insufficient to charge the battery. However, as seen in Figure 7, charging takes place during the positive cycle where the voltage has a peak value of 8.1V. The voltage waveforms show a voltage of 2.74 volts at the battery terminals, and an average load current of 169 mA after about 10 minutes of charging. In reality, the current flow into the battery is discontinuous.

The charge current starts at a value of about 200 mA and drops over time as the battery voltage rises. The charge current would also fluctuate slightly in line with the mains supply fluctuations. Hence, the charge time cannot be calculated precisely. Taking a nominal charge current of 170 mA and charge efficiency of about 80%, the total time to charge a 2000 mH battery is expected to take 14 hours.

CONTROL STRATEGY AND ALGORITHM

The performance of the charger based on the proposed concept is affected by the following parameters:

- Component tolerances
- Poor transformer regulation
- Measurement errors in the ADC
- Environmental effects such as the mains voltage fluctuation and temperature
- The large ripple due to the half-wave rectifier

The impact of component and environmental variations can be minimized by developing an algorithm based on statistical techniques. Details of this technique will be discussed in the subsequent sections. The key parameter, the ADC values of the voltage at the battery terminals, is characterized using statistical techniques to develop a robust algorithm. For large volume production, it is recommended that this parameter be refined using larger samples.

FIGURE 5: STATE DIAGRAM OF CHARGER ALGORITHM

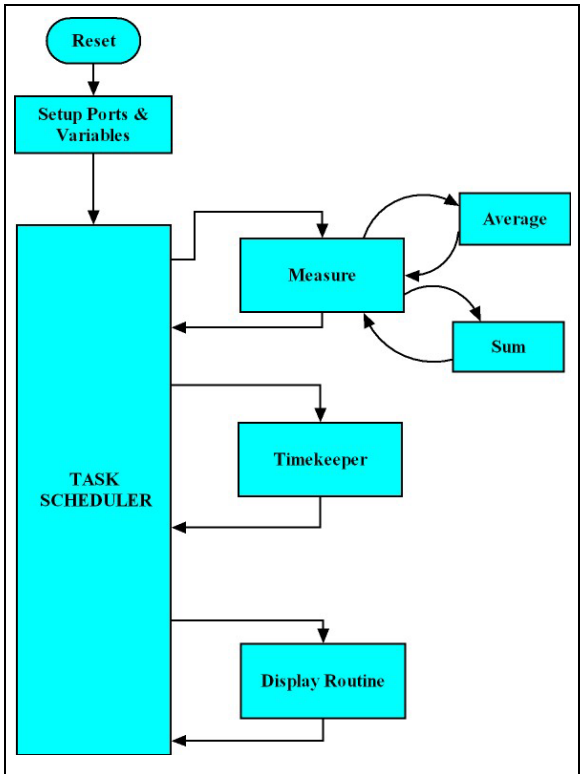

© Adapted with permission of the copyright owner Elsevier B.V.

DESCRIPTION OF THE CONTROL STRATEGY

The control strategy is based on a cooperative multitasking state machine. Discussion of a multitasking state machine is outside the scope of this application note, and the references at the end of this application note provide more details. The task scheduler employs a round-robin task management mechanism, and transfers control to the other tasks in a sequential manner, as all tasks have equal priority. However, some tasks were executed only if certain time constraints were met. For instance, ADC measurements were taken at certain time intervals. Figure 5 outlines the key modules of the state machine.

The following features of the PIC10F222 required a unique arrangement in the implementation of the different software modules:

- Program Memory: 512 words
- Data Memory: 23 bytes
- Program Counter: 9 bits wide

In a CALL instruction, PC<8> is cleared and, therefore, calls or computed jumps are limited to the first 256 locations. In a GOTO statement, bits 8:0 allow access to the entire 512 locations. The Stack size of two limits the usage of nested routines and imposed additional constraints on CALL instructions.

Brown-out Reset is not available and would require an external circuitry. In this design, this feature has been omitted for simplicity and cost consideration.

Timing – Timer0 provides the system timing tick of one millisecond. The countdown rollover is detected by checking the timer's contents. If the countdown occurs when the PIC device is executing some other task, the countdown will be missed.

CODE DEVELOPMENT

Relocatable code using Microchip's assembler, MPASM™, is used to implement the control algorithm. This facilitates modular and reusable code development. The specific modules forming the different tasks are shown in Figure 5. Additional sub-modules (e.g., averaging algorithm), add to the flexibility. However, the constraints imposed for the CALL statements limit the number of independent modules. The code sections, which are automatically assigned by the linker, did not allow efficient utilization of the program memory.

The constraints imposed by the linker and the CALL statements are overcome by:

- Creating non-reusable modules within a major module (source file) in conjunction with GOTO statements. Figure 6 shows an example of the actual implementation of the code in the form of non-reusable modules.
- Manually assigning the code-sections for the reusable and non-reusable modules.

FIGURE 6: TASK SCHEDULER

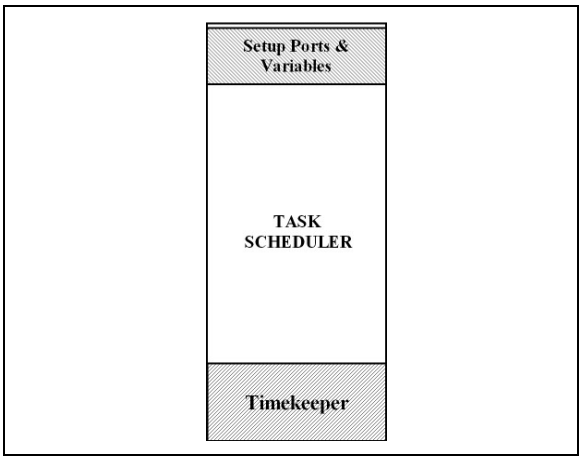

SOFTWARE MODULE

A brief description of the key software modules is given in the sections below.

TASK SCHEDULER

The task scheduler employs a round-robin task management mechanism and transfers control to the other tasks in a sequential manner. This is referred to as cooperative multitasking and depicted in Figure 5. When first plugged to the mains the LEDS are switched on for a period of about one minute to indicate to the user that the charger is working. Full execution of the multi-tasking algorithm begins after this delay. All tasks have equal priority and control is returned to the task scheduler at the end of each task. A software-based task prioritization is possible, but was deemed unnecessary.

The task scheduler also decides if the charge cycle has been completed and sets the appropriate flag in the Charge_Status_Register.

TIME KEEPER

The single timer in the PIC10F222 was configured to provide a system timer tick every millisecond and the timer rollover is confirmed by checking the zero flag in the STATUS register. A number of counters are used to multiply this one millisecond tick into 100 milliseconds, seconds, minutes and hours in the timekeeper module.

100 millisecond Counter	Used to implement the LED flashing rate for a Fault condition
1 Second Counter	Used to implement the LED flashing rate to indicate charge completion
1 Hour Counter	Used to implement the stipulated charge time.

It is not possible to ensure that the timer tick is detected on every occasion and ensure that the co-dependent timer counters are incremented at the right time. If the rollover occurs when the program is executing another task, for example, the MEASURE routine, the timer rollover will be missed. Moreover, the execution time of the MEASURE routine is also dependent on certain conditions within this module. However, this error in timing is insignificant in comparison to the charging duration of 14 hours and ADC sampling interval of one to two minutes.

MEASURE

This module is responsible for measuring the battery voltages at both channels. Due to the long time response of the charging process, a measurement every minute or more is sufficient. The presence of the batteries in each channel is checked regularly in case the battery was removed or the battery was shorted. If no batteries are detected, then no further measurement will take place and the corresponding display routine will display the “no battery” status. The designer should ensure that the mechanical design of the charger will prevent the end user from inserting or replacing the batteries while the charger is plugged into a wall socket.

The PIC device takes 16 readings in a sequential manner on each channel and an averaging algorithm is used to filter any noise. The averaged voltage values for both channels are stored for subsequent processing.

The stored voltage values are checked for possible Fault conditions. Flags related to a Fault condition are set if the measured voltages fall outside the predefined boundaries. The boundaries and the techniques to detect faults or the battery status were defined by characterizing the variation of the measured voltages using statistical techniques. A brief description of the statistical techniques employed is explained in the subsequent sections.

DISPLAY ROUTINE

This module is responsible for flashing the LEDs in a manner outlined in Table 1. On entry to this routine, pin GP2 is set to Low. GP0 and GP1 are set to digital output. The decision to switch on a specific LED and/or select an appropriate LED flashing rate is based on the flags in the two registers, Charge_Status_Flag and the Time_Keeper_Flag. These flags are set or cleared in the timekeeper or measure modules.

PROTEUS AND MPLAB® SIM

The simulation was carried out in Proteus and MPLAB SIM. Proteus is a package that allows schematic capture, interactive simulation and PCB layout. It can be used as a stand-alone package or via MPLAB® IDE. Typically, MPLAB IDE will generate error messages related to syntax. However, Proteus displays errors related to device configuration settings (e.g., ADC configuration errors, etc.). It also has a range of virtual instruments such as oscilloscopes, voltage and current probes. Proteus proved to be an invaluable tool that allowed about 60% of the software development and testing to be completed without actually wiring the circuit. MPLAB SIM allowed the Analog-to-Digital Converter and timing issues to be verified before debugging the code using the debug header AC162070.

TESTING

Each module was developed with the primary code and a test code integrated into the source file. Subsequently, all the modules were combined and tested in conjunction with a test module. However, the memory constraints explained earlier limited this approach. As such, the final phase of testing had to be carried out using the debug header.

EXPERIMENTAL RESULTS

Figure 7 shows the charge current, output voltage of the transformer and the voltage at the battery terminals. These values correlate to the calculated values reasonably well. The variation was due to a slight distortion in the waveform at the transformer output terminals. This distortion may be due to the imperfect mains waveforms or due to the step-down transformer’s characteristics.

FIGURE 7: VOLTAGES AND CURRENT PROFILES OF THE CHARGER

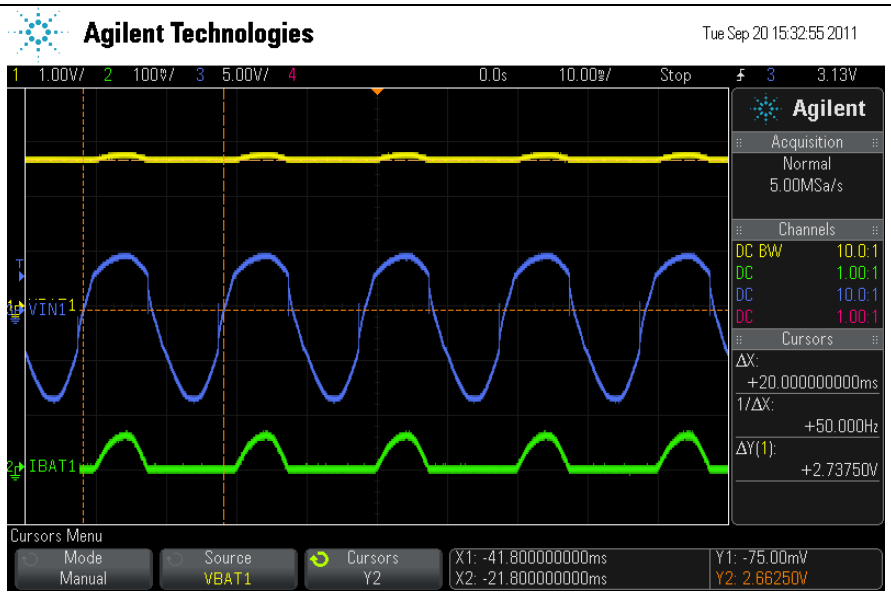

VOLTAGE MEASUREMENT

The accuracy of the voltage measurements using the PIC10F222 ADC is crucial to the successful implementation of the charger algorithm. The charger's voltage has a certain amount of ripple when the battery is present and a significant amount of ripple when the battery is not present. The boundary conditions to determine the battery present, no battery or primary cells are affected by the parameters described previously, which are outside the designer's control. However, the ADC resolution and error can be quantified.

ADC ERROR

The maximum ADC errors from the data sheet are shown below.

EIL = Integral error = ±1.5LSB

EDL = Differential error = -1 <EDL< +1.5LSB

EOFF = Offset error = ±1.5LSB

EGN = Gain error = ±1.5LSB

EQUATION 5:

$$\text{The cumulative error} = \sqrt{EIL^2 + EDL^2 + EOFF^2 + EGN^2}$$
$$= \sqrt{1.5^2 + 1.5^2 + 1.5^2 + 1.5^2}$$
$$= 3\ bits$$

A pair of discharged NiMH cells gave an average voltage of 2.72 volts after a charge time of 15 minutes. Random voltage measurements carried out by the PIC device correlated well to the voltmeter readings. The sample size of 20 measurements taken randomly was considered statistically significant for this application note.

Due to the small charge current, the voltage rise over time was slow and reached a peak voltage of 2.92 volts after 14 hours. Figure 8 shows the voltage and current profile of a trickle charger that was plugged into the mains socket and run for about 15 hours. The charge current profile reflects the mains voltage disturbances.

FIGURE 8: CHARGE PROFILE OF THE TRICKLE CHARGER

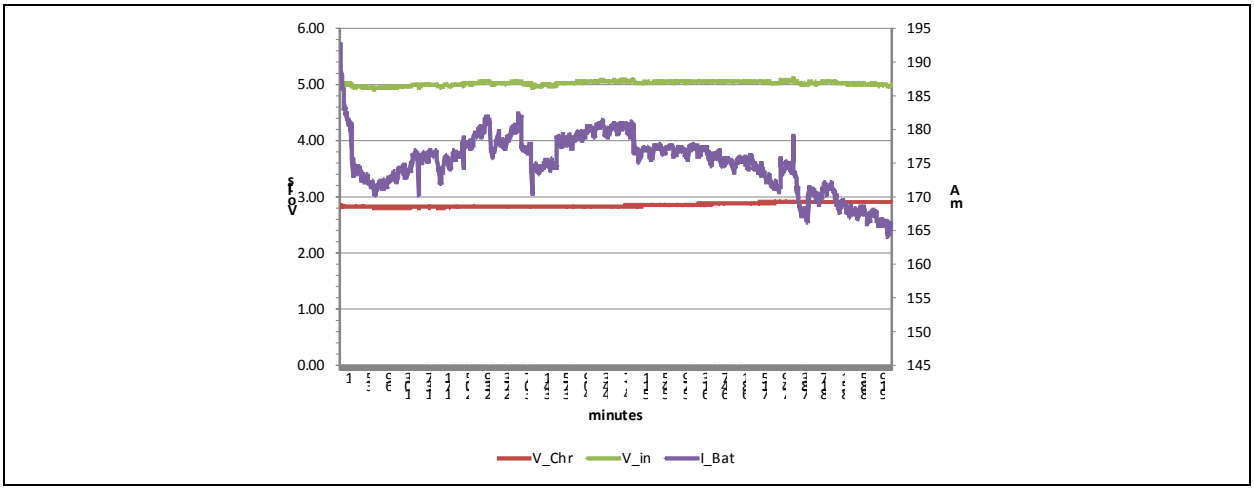

Statistical Analysis

The correct measurement of the voltage affects the successful implementation of the algorithm in this product. The variability introduced by a range of factors outlined in earlier sections represents a significant challenge in light of the cost constraints without compromising the quality and performance. Hence, it is necessary to measure and analyze this variation using statistical techniques. This approach will minimize producibility issues related to design, process and material variation.

The reader is encouraged to refer to the listed references for additional information on the application of statistical techniques to develop a robust product.

The proposed technique is consistent with Process (Machine) Capability Analysis used to quantify the process variation and in this case, was adopted to determine the optimum boundary values for the algorithm. Typically, a product that meets the six sigma process capability standard is considered acceptable. The parameter (variable) in this case is the ADC value representing the voltage at the battery terminals.

A brief explanation of the following statistical terms is required to explain the application of Statistical Analysis of the key variable, namely the ADC values.

Nominal	The calculated or design value.
Delta	Tolerance.
Lower Specification Limit (*LSL*)	The nominal value minus the tolerance.
Upper Specification Limit (*USL*)	The nominal value plus the tolerance.
Mean (μ)	The central tendency of the variable.
Standard deviation (σ)	Also referred to as sigma, is a measure of the variation.
Process capability Index (C_{pk})	A measure of the process capability. A value of 1.33 signifies conformance to the six sigma standards, required for commercial products in non-safety critical applications.

VOLTAGE MEASUREMENT WITH GOOD NiHM BATTERIES

The battery voltage is 2.72 volts after about 15 minutes of charging. 2.72 volts is equivalent to the ADC result of 211 using the V_{DD} of 3.3 volts as reference. As such, the specification for the voltage is given by:

Nominal = 211

Delta = 3 (this is the ADC error)

The measured values were analyzed and plotted using an evaluation version of the *STATISTICA*, a statistical analysis software from Statsoft Inc. The statistical distribution and computed process values are shown in Figure 9. These did not meet the normal distribution requirements and the calculated process capability index C_{pk} did not meet the six sigma standards. An abnormal characterization technique due to Johnson-Pearson also did not provide an acceptable C_{pk}.

FIGURE 9: STATISTICAL DISTRIBUTION WITHOUT CORRECTION

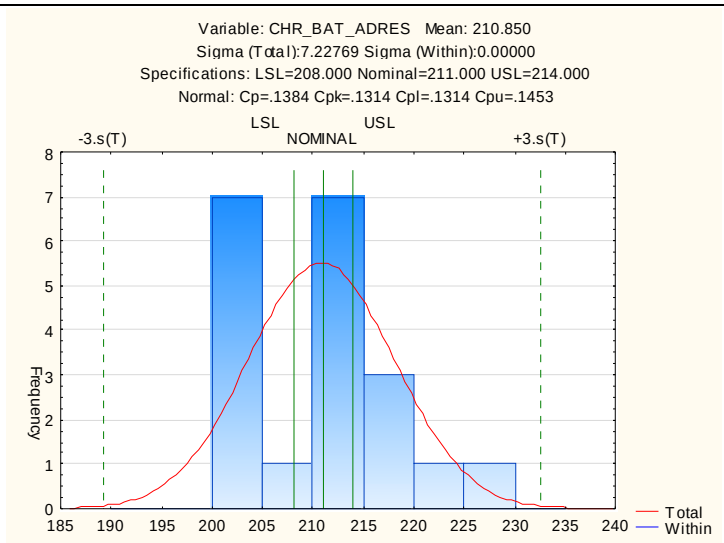

© Created with permission from Statsoft Inc.

TABLE 2: PROCESS VALUES WITHOUT CORRECTION

-3.000 *Sigma=189.167 +3.000 *Sigma=232.533	
Parameter	**Value**
Lower Specification Limit	208.0000
Nominal Specification	211.0000
Upper Specification Limit	214.0000
CP (potential capability)	0.1384
Sigma	7.22769
CR (capability ratio)	7.2277
CPK (demonstrated excellence)	0.1314
CPL (lower capability index)	0.1314
CPU (upper capability index)	0.1453
K (non-centering correction)	0.0500
CPM (potential capability II)	0.1383
© Created with permission from Statsoft Inc.	

TABLE 3: PROBABILITY OF FAILURE-ESTIMATION

	Observed	Percent – Observed	Expected	Percent – Expected
Above USL:	5	25.00000	6.62964	33.14822
Below LSL:	7	35.00000	6.93347	34.66735
Total	12	60.00000	13.56311	67.81557

© Created with permission from Statsoft Inc.

The chances of the measurement values exceeding the specification boundaries can be estimated and is shown in Table 3. Given the significant potential for failures, the solution was to extend the lower and upper specification to the six sigma standard which would ensure a C_{pk} of 1.33 or higher.

Based on Figure 9, the specification limits were redefined as follows:

Lower Specification Limit (LSL) = 185

Upper Specification Limit (USL) = 235

Figure 10 shows the results from the redefined specification limits.

FIGURE 10: REDEFINED SPECIFICATION LIMITS

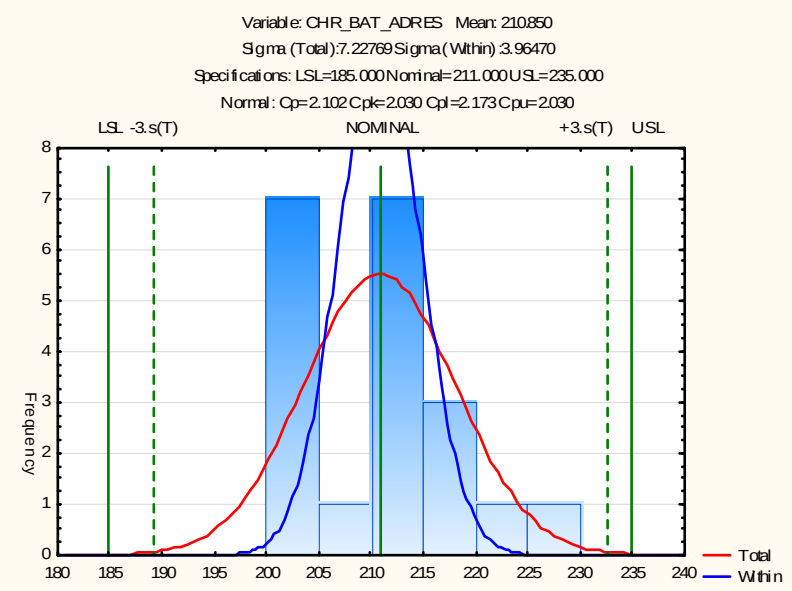

© Created with permission from Statsoft Inc.

TABLE 4: PROCESS VALUES WITH REDEFINED SPECIFICATION LIMITS

	Normal – Distribution
Lower Specification Limit	185.0000
Nominal Specification	211.0000
Upper Specification Limit	235.0000
Lower Perc. Value: .135	198.9559
Median (50%) Value: 50.000	210.8500
Upper Perc. Value: 99.865	222.7441
CP (potential capability)	2.1019
sigma	7.22769
CR (capability ratio)	0.4758
CPK (demonstrated excellence)	2.0304
CPL (CP, lower)	2.1733
CPU (CP, upper)	2.0304
K (non-centering correction)	0.0340
© Created with permission from Statsoft Inc.	

TABLE 5: PROBABILITY OF FAILURE WITH REDEFINED SPECIFICATION LIMITS

	Observed	Percent – Observed	Expected	Percent – Expected
Above USL:	0	0.00	0.008338	0.041691
Below LSL:	0	0.00	0.003482	0.017410
Total	0	0.00	0.011820	0.059101
© Created with permission from Statsoft Inc.				

The revised C_{pk} value exceeded the six sigma standards. The probability of some measurements exceeding the specification boundaries is shown in Table 3. The small probability of failure is acceptable and the revised LSL and USL were used to define the boundary conditions in the algorithm.

VOLTAGE MEASUREMENT WITHOUT BATTERIES

In order to detect that the batteries are not present, accurate measurement of the voltage at the battery terminals is important. The voltage waveform at the battery terminals without any inserted batteries is shown in Figure 11. An algorithm based on this waveform will be complicated.

FIGURE 11: VOLTAGE WAVEFORM AT BATTERY TERMINALS

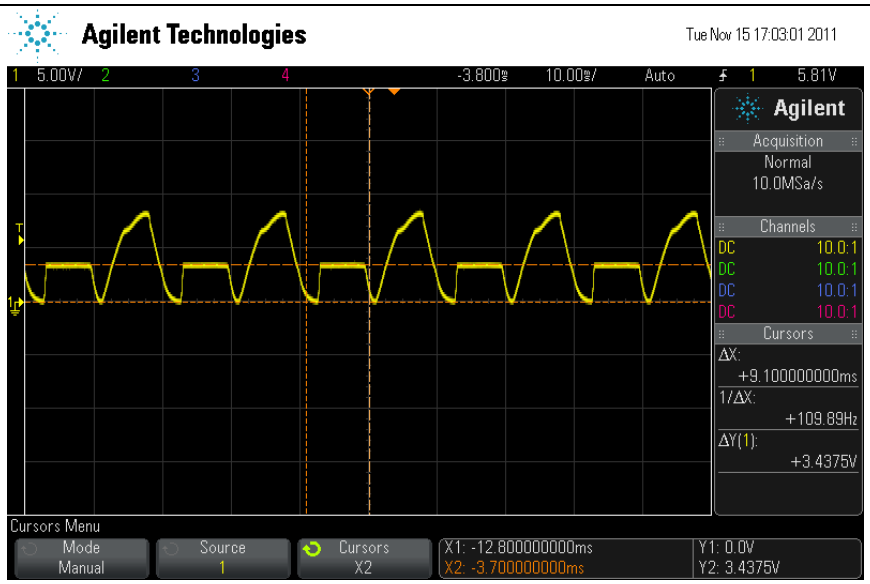

The irregular waveform, due to the PIC10F222 internal clamping diode, was removed when the PIC device I/O pin was set to analog together with a resistor between the I/O pin and ground. The resulting half-wave rectifier waveform is shown in Figure 12.

FIGURE 12: VOLTAGE WAVEFORM WITHOUT BATTERIES

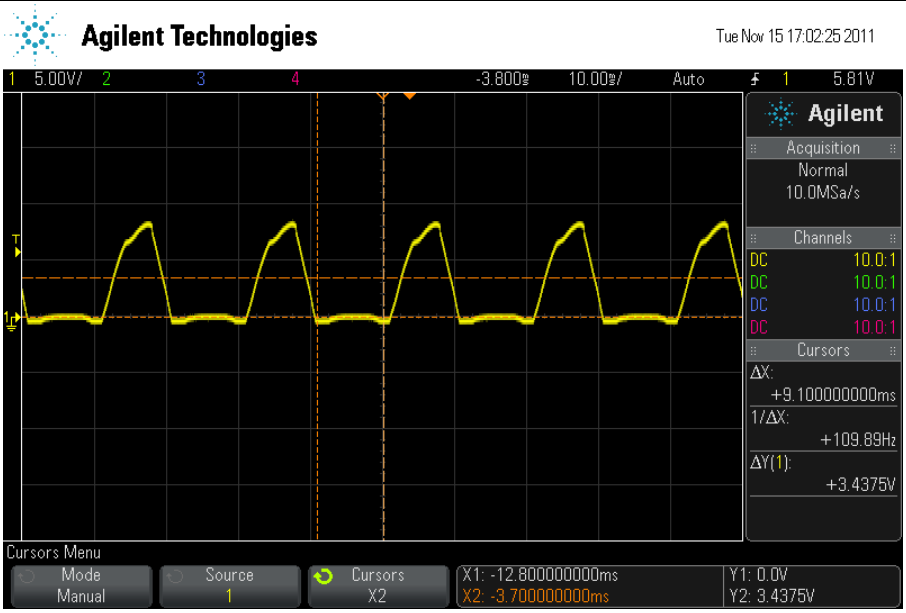

The statistical distribution of a random sampling of the voltage without the batteries is shown in Figure 13. The theoretical specification based on “no batteries” and factoring in the ADC error gives the following specification:

- Nominal: 0
- Upper Specification Limit (USL): 3

It is obvious that this distribution is abnormal and the spread of the data-points would not lend itself well to the six sigma process control concept outlined earlier.

FIGURE 13: STATISTICAL DISTRIBUTION WITHOUT BATTERIES

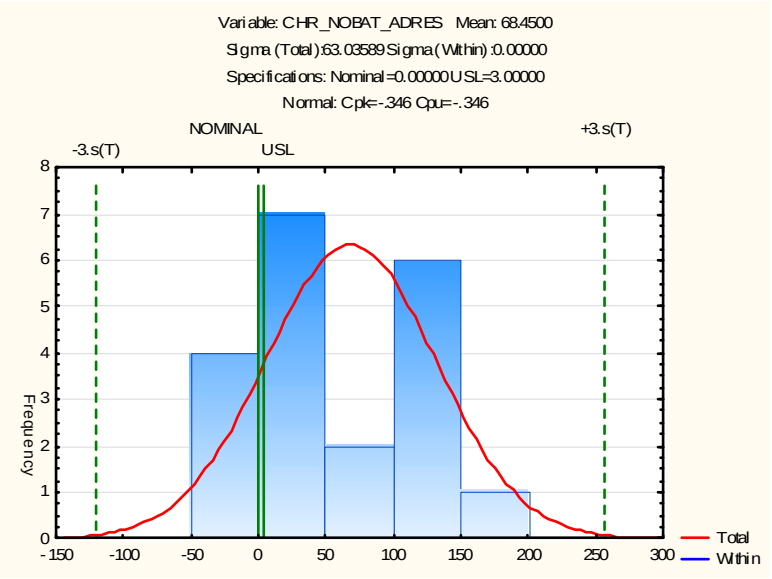

© Created with permission from Statsoft Inc.

NO BATTERY AND FAULT DETECTION LOGIC

Figure 6 allows easy visualization and facilitates development of a suitable algorithm to detect the abnormal conditions. A standard deviation of 7.23 based on test measurements is used to tabulate the spread. The typical conditions are:

- No battery
- Battery present – Discharged Battery
- Battery present – Fully charged Battery
- Primary battery
- Shorted or defective battery

The decision logic to detect the conditions above is described in conjunction with Figure 14.

TABLE 6: STATISTICAL SPREAD OF THE ADC MEASUREMENTS

	Battery Low Charge	Battery Fully Charged	No Battery	Primary Cell
0				
7.23				
14.46				
21.69				
28.92				
36.15				
43.38				
50.61				
57.84				
65.07				
72.3				
79.53				
86.76				
93.99				
101.22				
108.45				
115.68				
122.91				
130.14				
137.37				
144.6				
151.83				
159.06				
166.29				
173.52				
180.75				
187.98				
195.21				
202.44				
209.67				
216.9				
224.13				
231.36				
238.59				
245.82				
253.05				
260.28	This region is outside the 8-bit limit and will return 0xFF			
267.51				
274.74				
281.97				

NO BATTERY DETECTION

Since a “no battery” condition can result in values across the entire range of the ADC values, as seen in Table 6, the presence of a voltage below the battery absence value is taken as “no battery” and the corresponding LED is turned off. In the current firmware, the decimal value 50 was taken as a battery absent value. No further readings are taken on this channel unless the charger is reset by recycling power.

FAULT CONDITION

Primary batteries, fully charged batteries and shorted batteries represent Fault conditions. The overlap in voltage values between primary and fully charged batteries make it difficult to distinguish these two types of batteries using the current algorithm. To prevent spurious Fault conditions being recorded, the algorithm takes repeated samples at regular intervals for a period of time and a corresponding counter is incremented as shown in Figure 14. A fault is reported only after repeated Fault conditions have been detected over this period. The acceptable range for a good battery is values between V_{min} and V_{max}.

V_{min} – Minimum Battery Voltage

V_{max} – Maximum Battery Voltage

PRIMARY BATTERIES

Primary batteries are rated at 1.5 volts, and adding two batteries in series would always result in the maximum charger voltage, in some cases in excess of 3.0V. The ADC will a return value of 0xFF. A discharged primary battery would have a value lower then 1.5V. However, when charged even at low charge currents, the terminal voltage would quickly rise. If the battery is not removed, the pressure build-up will rupture the seals, causing the electrolyte to leak.

FULLY CHARGED BATTERIES

In a fast charger, the inflection of the voltage profile corresponding to full charge is detected and the charger will reduce the current to a trickle charge value and display that the battery is already charged. However, in this concept, the low charge current will not return discernible inflection points. Hence, a simple logic indicating a fault was implemented.

If the voltage is still higher than the predefined threshold for V_{max} over the time frame defined by the FAULT_COUNTER_HIGH register, then the fault flag is set.

The current algorithm is unable to distinguish between a primary and a fully charged NiMH cell because the voltages overlap. Yet, when the end-user sees a fault indication on the LED for a fully charged NiMH cell, this would be a reasonable alert on the battery status.

SHORTED BATTERIES

Batteries which are internally shorted would have 0V or voltage levels below 0.9V, even after being charged for some time. The charger checks for the battery status one minute after Power On, and then subsequently at regular intervals defined in the software. As there is no absolute method to distinguish between a shorted battery and a discharged battery, the algorithm monitors the voltage for a considerably longer period of time than the condition for primary/fully charged batteries.

If the voltage is still lower than the predefined threshold for V_{min} over the time frame defined by the FAULT_COUNTER_LOW register, then a fault flag is set. This feature facilitates a fully discharged NiMH battery to be charged without spurious faults being triggered.

FIGURE 14: DECISION LOGIC FOR FAULTS

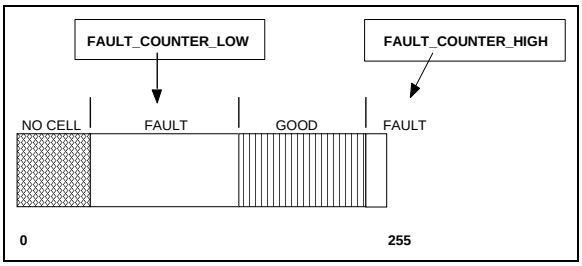

PCB LAYOUT

A small single layer PCB using easily available SMT components and a PIC10F222 (SOT23 size) can be implemented in a commercial trickle charger as shown in Figure 15. Figure 16 shows the components placement.

FIGURE 15: PCB OF THE TRICKLE CHARGER – TOP LAYER

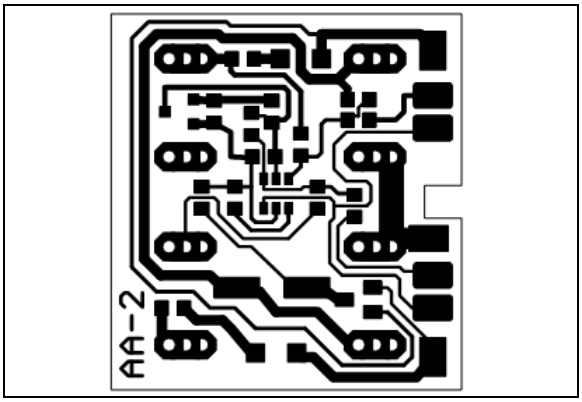

FIGURE 16: COMPONENTS PLACEMENTS – TOP LAYER

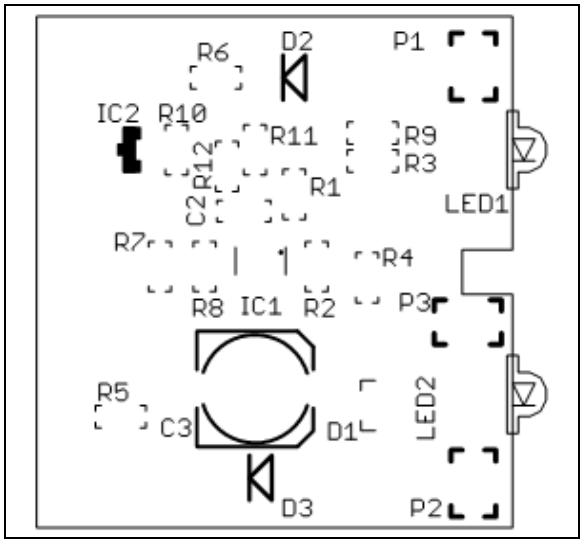

RESULTS AND DISCUSSIONS

This application note describes the design and implementation of a low-cost, intelligent trickle charger. The use of statistical techniques to facilitate the development of a robust algorithm was explored. This technique can be enhanced by incorporating more complex fault detection algorithm in a future design. The modular firmware based on relocatable code facilitates scalability.

A 2000 mAH battery will need about 14 hours to charge fully at 0.1C using the 50/60 Hz transformer-based charger, bearing in mind the mains voltage fluctuations and the reduction in charge current as the battery voltage rises.

Currently, batteries with 2600 mAH rating are available, and increasing the charge current using a conventional 50/60 Hz transformer may not be aesthetically or weight-wise feasible. A switched-mode power supply will be required. The safety compliance, EMI compliance and interference to the PIC10F within the space constraints of such a charger would have to be investigated. The added benefit is the universal mains input for a world traveller.

CONCLUSIONS

The viability of adding intelligence to a low-cost NiMH charger was demonstrated using the PIC10F222.

MEMORY REQUIREMENTS

Program memory: 340 words

Data memory: 17 bytes

ACKNOWLEDGEMENT

Microchip appreciates the support provided by Hahnel Industries, Bandon, Co Cork, Ireland.

REFERENCES

[1] *Journal of Power Sources 112* (2002)298-306 – *An experimental and modelling study of isothermal charge/discharge behaviour of commercial NiMH cells* – Y.H.Pan, V.Srinivasan, C.Y.Wang – Elsevier B.V

[2] *Embedded Multitasking. Newnes Publishing* – Keith Curtis

[3] *Six Sigma Producibility Analysis and Process Characterization* – Mikel J.Harry, J.Ronald Lawson

[4] *STATISTICS – Methods and Applications*, Statsoft Ltd. – Thomas Hill, Pawel Lewicki

[5] StatSoft, Inc. (2012). *STATISTICA (Data Analysis Software System), version10,* www.statsoft.com

[6] *Pergamon, Electrochimica Acta 44(1999) 4525 – 4541, Modeling Discharge and Charge Characteristics of Nickel-Metal Hydride Batteries* – W.B.Gu, C.Y.Wang, S.M.Li, MM.Geng, B.Y.Liaw

Microchip Documents (http://www.microchip.com)

[7] AN960, "*New Components and Design methods Bring Intelligence to Battery Charger Applications*" – Terry Cleveland, Catherine Vannicola, Microchip Technology Inc.

[8] AN1088, "*Selecting the Right Battery System for Cost Sensitive Portable Applications While Maintaining Excellent Quality*" – Brian Chu, Microchip Technology Inc.

[9] AN1384, "*NiMH Battery Charger Application Library*" – Mihnea Rosu-Hamzescu; Microchip Technology Inc.

[10] AN1137, "*Using the MCP1631 Family to Develop Low-Cost Battery Chargers*" – Terry Cleveland; Microchip Technology Inc.

NOTES:

Note the following details of the code protection feature on Microchip devices:

- Microchip products meet the specification contained in their particular Microchip Data Sheet.
- Microchip believes that its family of products is one of the most secure families of its kind on the market today, when used in the intended manner and under normal conditions.
- There are dishonest and possibly illegal methods used to breach the code protection feature. All of these methods, to our knowledge, require using the Microchip products in a manner outside the operating specifications contained in Microchip's Data Sheets. Most likely, the person doing so is engaged in theft of intellectual property.
- Microchip is willing to work with the customer who is concerned about the integrity of their code.
- Neither Microchip nor any other semiconductor manufacturer can guarantee the security of their code. Code protection does not mean that we are guaranteeing the product as "unbreakable."

Code protection is constantly evolving. We at Microchip are committed to continuously improving the code protection features of our products. Attempts to break Microchip's code protection feature may be a violation of the Digital Millennium Copyright Act. If such acts allow unauthorized access to your software or other copyrighted work, you may have a right to sue for relief under that Act.

Trademarks

ISBN: 9781620764886

QUALITY MANAGEMENT SYSTEM
CERTIFIED BY DNV
ISO/TS 16949

Microchip received ISO/TS-16949:2009 certification for its worldwide headquarters, design and wafer fabrication facilities in Chandler and Tempe, Arizona; Gresham, Oregon and design centers in California and India. The Company's quality system processes and procedures are for its PIC® MCUs and dsPIC® DSCs, KEELOQ® code hopping devices, Serial EEPROMs, microperipherals, nonvolatile memory and analog products. In addition, Microchip's quality system for the design and manufacture of development systems is ISO 9001:2000 certified.

Worldwide Sales and Service

AMERICAS

Corporate Office
2355 West Chandler Blvd.
Chandler, AZ 85224-6199
Tel: 480-792-7200
Fax: 480-792-7277
Technical Support:
http://www.microchip.com/support
Web Address:
www.microchip.com

Atlanta
Duluth, GA
Tel: 678-957-9614
Fax: 678-957-1455

Boston
Westborough, MA
Tel: 774-760-0087
Fax: 774-760-0088

Chicago
Itasca, IL
Tel: 630-285-0071
Fax: 630-285-0075

Cleveland
Independence, OH
Tel: 216-447-0464
Fax: 216-447-0643

Dallas
Addison, TX
Tel: 972-818-7423
Fax: 972-818-2924

Detroit
Farmington Hills, MI
Tel: 248-538-2250
Fax: 248-538-2260

Indianapolis
Noblesville, IN
Tel: 317-773-8323
Fax: 317-773-5453

Los Angeles
Mission Viejo, CA
Tel: 949-462-9523
Fax: 949-462-9608

Santa Clara
Santa Clara, CA
Tel: 408-961-6444
Fax: 408-961-6445

Toronto
Mississauga, Ontario, Canada
Tel: 905-673-0699
Fax: 905-673-6509

ASIA/PACIFIC

Asia Pacific Office
Suites 3707-14, 37th Floor
Tower 6, The Gateway
Harbour City, Kowloon
Hong Kong
Tel: 852-2401-1200
Fax: 852-2401-3431

Australia - Sydney
Tel: 61-2-9868-6733
Fax: 61-2-9868-6755

China - Beijing
Tel: 86-10-8569-7000
Fax: 86-10-8528-2104

China - Chengdu
Tel: 86-28-8665-5511
Fax: 86-28-8665-7889

China - Chongqing
Tel: 86-23-8980-9588
Fax: 86-23-8980-9500

China - Hangzhou
Tel: 86-571-2819-3187
Fax: 86-571-2819-3189

China - Hong Kong SAR
Tel: 852-2401-1200
Fax: 852-2401-3431

China - Nanjing
Tel: 86-25-8473-2460
Fax: 86-25-8473-2470

China - Qingdao
Tel: 86-532-8502-7355
Fax: 86-532-8502-7205

China - Shanghai
Tel: 86-21-5407-5533
Fax: 86-21-5407-5066

China - Shenyang
Tel: 86-24-2334-2829
Fax: 86-24-2334-2393

China - Shenzhen
Tel: 86-755-8203-2660
Fax: 86-755-8203-1760

China - Wuhan
Tel: 86-27-5980-5300
Fax: 86-27-5980-5118

China - Xian
Tel: 86-29-8833-7252
Fax: 86-29-8833-7256

China - Xiamen
Tel: 86-592-2388138
Fax: 86-592-2388130

China - Zhuhai
Tel: 86-756-3210040
Fax: 86-756-3210049

ASIA/PACIFIC

India - Bangalore
Tel: 91-80-3090-4444
Fax: 91-80-3090-4123

India - New Delhi
Tel: 91-11-4160-8631
Fax: 91-11-4160-8632

India - Pune
Tel: 91-20-2566-1512
Fax: 91-20-2566-1513

Japan - Osaka
Tel: 81-66-152-7160
Fax: 81-66-152-9310

Japan - Yokohama
Tel: 81-45-471- 6166
Fax: 81-45-471-6122

Korea - Daegu
Tel: 82-53-744-4301
Fax: 82-53-744-4302

Korea - Seoul
Tel: 82-2-554-7200
Fax: 82-2-558-5932 or
82-2-558-5934

Malaysia - Kuala Lumpur
Tel: 60-3-6201-9857
Fax: 60-3-6201-9859

Malaysia - Penang
Tel: 60-4-227-8870
Fax: 60-4-227-4068

Philippines - Manila
Tel: 63-2-634-9065
Fax: 63-2-634-9069

Singapore
Tel: 65-6334-8870
Fax: 65-6334-8850

Taiwan - Hsin Chu
Tel: 886-3-5778-366
Fax: 886-3-5770-955

Taiwan - Kaohsiung
Tel: 886-7-536-4818
Fax: 886-7-330-9305

Taiwan - Taipei
Tel: 886-2-2500-6610
Fax: 886-2-2508-0102

Thailand - Bangkok
Tel: 66-2-694-1351
Fax: 66-2-694-1350

EUROPE

Austria - Wels
Tel: 43-7242-2244-39
Fax: 43-7242-2244-393

Denmark - Copenhagen
Tel: 45-4450-2828
Fax: 45-4485-2829

France - Paris
Tel: 33-1-69-53-63-20
Fax: 33-1-69-30-90-79

Germany - Munich
Tel: 49-89-627-144-0
Fax: 49-89-627-144-44

Italy - Milan
Tel: 39-0331-742611
Fax: 39-0331-466781

Netherlands - Drunen
Tel: 31-416-690399
Fax: 31-416-690340

Spain - Madrid
Tel: 34-91-708-08-90
Fax: 34-91-708-08-91

UK - Wokingham
Tel: 44-118-921-5869
Fax: 44-118-921-5820

11/29/11